

12

ADA018871

STRESS OPTICAL PROPERTIES OF SOLIDS  
IN THE 1 TO 20 MICRON WAVELENGTH REGION

by

John P. Szczesniak and John C. Corelli

Department of Nuclear Engineering

Rensselaer Polytechnic Institute

Troy, NY 12181

FINAL REPORT

1 August 1973 through 30 June 1975

July 1975

Approved for public release; distribution unlimited

Prepared For

AIR FORCE CAMBRIDGE RESEARCH LABORATORIES

AIR FORCE SYSTEMS COMMAND

UNITED STATES AIR FORCE

HANSCOM AFB, MASSACHUSETTS 01731

DDC  
JAN 5 1976

S/c 408229

Qualified requestors may obtain additional copies from the Defense Documentation Center. All others should apply to the National Technical Information Service.

LA

Unclassified

SECURITY CLASSIFICATION OF THIS PAGE (When Data Entered)

REPORT DOCUMENTATION PAGE		READ INSTRUCTIONS BEFORE COMPLETING FORM	
1. REPORT NUMBER <b>18</b> AFCRL-TR-75-0476	2. GOVT ACCESSION NO.	3. RECIPIENT'S CATALOG NUMBER <b>9</b>	
4. TITLE (and Subtitle) <b>6</b> STRESS OPTICAL PROPERTIES OF SOLIDS IN THE 1 TO 20 MICRON WAVELENGTH REGION.		5. TYPE OF REPORT & PERIOD COVERED Final Report 1 August 1973 - 30 June 1975	
7. AUTHOR(s) <b>10</b> John P. Szczesniak John C. Corelli		6. PERFORMING ORG. REPORT NUMBER	
9. PERFORMING ORGANIZATION NAME AND ADDRESS Rensselaer Polytechnic Institute Department of Nuclear Engineering Troy, NY 12181		10. PROGRAM ELEMENT, PROJECT, TASK AREA & WORK UNIT NUMBERS 3326-08-01 62601F	
11. CONTROLLING OFFICE NAME AND ADDRESS Air Force Cambridge Research Laboratories Hanscom AFB, Massachusetts 01731 Contract Monitor-Carl A. Pitha/LQS		12. REPORT DATE <b>11</b> July 1975	
14. MONITORING AGENCY NAME & ADDRESS (if different from Controlling Office) <b>16</b> AF-3326 <b>17</b> 332608		13. NUMBER OF PAGES 29 <b>12</b> 33 p.	
16. DISTRIBUTION STATEMENT (of this Report) A-Approved for public release; distribution unlimited.		15. SECURITY CLASS. (of this report) Unclassified	
17. DISTRIBUTION STATEMENT (of the abstract entered in Block 20, if different from Report)		15a. DECLASSIFICATION/DOWNGRADING SCHEDULE	
18. SUPPLEMENTARY NOTES			
19. KEY WORDS (Continue on reverse side if necessary and identify by block number) Stress Optic Coefficients Infrared wavelength region (1 to 12 microns) Birefringence and retardance Alkali Halides (KCl, KBr, KI, NaCl, etc.) Non-oxide Glasses (ZnS, ZnSe, SrF <sub>2</sub> , etc.)			
20. ABSTRACT (Continue on reverse side if necessary and identify by block number) The application of a variation of intensity method using static uniaxial compressive stress and polarized light to measure stress-induced birefringence in the infrared wavelength region (1 to 12 microns) is described. The measurements were made at 296°K for the following materials: KCl, KBr, KI, NaCl, LiF, ZnS, ZnSe and SrF <sub>2</sub> , CaF <sub>2</sub> , MgF <sub>2</sub> and a chalcogenide glass TI-1173 for the alkali halides the values of the stress optic coefficients obtained are in the range 1 to 4 Brewsters, while for the non-oxide glasses values			

DD FORM 1473  
1 JAN 73

EDITION OF 1 NOV 65 IS OBSOLETE  
S/N 0102-014-6601

SECURITY CLASSIFICATION OF THIS PAGE (When Data Entered)

408229

Handwritten initials/signature

CONTINUED

SECURITY CLASSIFICATION OF THIS PAGE(When Data Entered)

of 9 to 14 Brewsters were measured. Comparisons of measurements from experiments with a theoretical model which predicts the wavelength dispersion of stress birefringence cannot be fitted better than a factor of  $\approx 2$ .

APPROXIMATELY

SECURITY CLASSIFICATION OF THIS PAGE(When Data Entered)

## I. Preface

### A. General Description of Program, Objectives and Research Participants.

The use of materials as windows for transmitting light in the 1 to  $\sim$  11 micron wavelength region causes problems of beam stability when the light sources are high power ( $\geq$  1kw) lasers. In recent years high power CO<sub>2</sub> lasers (10.6 micron) have become available and the need has arisen to study and understand the interaction of intense light beams as they pass through the window. An important effect caused by the intense light beam is a distortion due to local thermal stress effects. In our program we studied one aspect of the problem, namely the measurement of the stress optic properties (at 300° K) of some alkali halide salts (KCL, KBr, KI, LiF, etc.) and non-oxide glasses (ZnSe, ZnS). In addition, we also examined the stress optic properties of CaF<sub>2</sub>, MgF<sub>2</sub> and SrF<sub>2</sub>.

Within the time limit of our program the wavelength region studied on most materials included the 1 to 12 micron range. The objectives of our program were as follows:

1. Extend the method of Michael<sup>(1)</sup> using phase retardation to determine the stress optical coefficient for the materials mentioned above from the 1 to 12 micron wavelength region.
2. Compare our measurements with theoretical calculations Bendow and Gianino<sup>(2)</sup> and compare our results at  $\lambda \lesssim 1\mu$  with experimental reports reported by other workers.

A search of the literature reveals that up to January 1, 1975 no other study had reported dispersion studies of the stress optic coefficient over the wavelength region covered in this study, namely for  $\lambda$  from 2 to 12 microns. Thus, the reader is advised initially that while there are no other measurements from 2 to 11 microns apart from the work of Pitha and Friedman<sup>(3)</sup> comparisons of experimental results with other workers for  $\lambda < 1$  micron is in fact possible.

The participants in this research program include Dr. John C. Corelli, part-time faculty member, during entire program; Dr. C. S. Chen, full-time research associate, 1 August 1973-1 March 1974; John P. Szczesniak, part-time throughout the entire program as a graduate student research assistant; David Cuddeback, NSF undergraduate

participant, summer, 1975.

B. Program Summary - Main findings and significance.

The single most important result of the program was the demonstration that the method of Michael<sup>(1)</sup> could be extended for measuring the stress optic coefficient of alkali halides and other non-oxide glasses to the wavelength region of 2 to 12 microns. In previous work the method of Michael was used to make the stress optic coefficient measurements only in the 0.5 to 1 micron wavelength.

We shall define the stress optic coefficients  $C_{\lambda}$  and  $C'_{\lambda}$  as used in this report as follows: For a cubic crystal with light ( $\vec{E}$ ) incident in a  $[100]$  direction and a uniaxial compressive stress ( $\vec{\sigma}$ ) applied in a  $[010]$  direction the stress optic coefficient or stress induced birefringence  $C_{\lambda}$  is defined as:

$$C_{\lambda} = \frac{1}{2} n_0^3 (q_{11} - q_{12}) \quad (1)$$

where  $n_0$  is the index of refraction, and the  $q_{11}$  and  $q_{12}$  are stress tensor components of the piezo-optic constants. The coefficient  $C'_{\lambda}$  is defined as:

$$C'_{\lambda} = \frac{n_0^3}{2} q_{44} \quad (2)$$

where now light is incident in the  $[001]$  direction and stress applied in a  $[110]$  direction. In Equation 2  $n_0$  is as defined in Equation 1 and  $q_{44}$  is a stress tensor component of the piezo-optic constant. More detailed discussion of the method for obtaining  $C_{\lambda}$  and  $C'_{\lambda}$  from the measurements and the relationship between the various stress optical constants the elasto-optical coefficients and the elastic strain components are given in the paper included in Appendix A of this report and will not be repeated here.

Main findings in the  $C_{\lambda}$  vs  $\lambda$  and  $C'_{\lambda}$  vs  $\lambda$  measurements.

1.  $C_{\lambda}$  exhibits wavelength dependence from 1 to 11 microns for KI, KCl, KBr, NaBr and NaCl. For LiF a slight increase in  $C_{\lambda}$  is observed as  $\lambda$  goes from 2 to 8 microns.
2.  $C'_{\lambda}$  for NaCl, KI and KBr shows no wavelength dispersion from  $\sim 1$  to 11 microns. The wavelength dependence given above are in general agreement with the predictions of the calculations of Bendow and Gianino<sup>(2)</sup>.

3. The  $C_{\lambda}$  for ZnSe and ZnS although larger in magnitude by a factor of  $\sim 3$  than for alkali halides also show no wavelength dependence from  $\sim 5$  to 11 microns which agree with the wavelength dependence predicted by calculation. <sup>(2)</sup>

Since the  $C_{\lambda}$  for  $\text{SrF}_2$ ,  $\text{MgF}_2$ ,  $\text{CaF}_2$  and TI -1173 glass were only measured at one wavelength no comparison with theory is possible until further experiments are performed.

## II. Experiments

In Appendix A we have given a detailed discussion of the theory of the measurement including the method of analysis to extract  $C_{\lambda}$  and  $C'_{\lambda}$  from the data. The discussion in Appendix A was applied to the wavelength region of 4 to 12 microns. When we made measurements in the 1 to 3 micron wavelength range the following modifications to the experimental arrangement (Fig. 2, Appendix A) were made. A fused silica prism replaced the NaCl prism in the monochromator, a tungsten filament lamp replaced the globar light source, the wire grid polarizers were replaced by Polaroid HR-polarizers which are useful in the 1 to 2.8 micron wavelength range. The wire grid polarizers are not effective for wavelengths smaller than about 4 microns in that they let through too much unwanted light  $\sim 5\%$ .

An additional modification made to the system for studying the 1 to 3 micron range was to use a PbS detector operated at a bias voltage of 45 volts DC. In order to increase the signal to noise ratio using the PbS detector the light chopping frequency was increased from 13 Hz (for the thermocouple detector) to 667 Hz. The above modifications were found to be adequate for most of the measurements of  $C_{\lambda}$  and  $C'_{\lambda}$  on the materials examined.

For purposes of completeness in this report we shall include a brief statement on an experiment which was not successful in the measurement of  $C_{\lambda}$  and  $C'_{\lambda}$  at 10.6 microns. In order to increase our signal at 10.6 microns a 20 watt  $\text{CO}_2$  laser (Hadron, Inc. Model 1020  $\text{CO}_2$  laser) was used as the light source. However, it was found that as the laser mode\* changed severe noise problems were encountered and this method had to be abandoned, as it was inferior to our globar

\*See bottom of Page 4.

light source stability. It is clear that a highly stable single mode laser must be used as the light source in these experiments in order to successfully measure  $C_{\lambda}$  and  $C'_{\lambda}$ .

### III. Stress Optic Results

#### A. Alkali Halides

The paper included in the Appendix A gives results on stress birefringence for KCl, KBr and LiF in the wavelength range from 4 to 12 microns. In this section we shall add to previously reported data by including results at 1.18 microns and 5 microns. In what follows the stress optic coefficient or retardance as given on the graphs is described in terms of "A" samples or "B" samples. The "A" samples mean stress is applied in a  $[001]$  direction and light is incident in a  $[100]$  direction giving  $C_{\lambda}$  as defined earlier. The "B" samples mean stress is applied in a  $[110]$  direction and light is passed through the samples in a  $[001]$  direction...giving  $C'_{\lambda}$  as defined earlier.

In Figure 1 we show the total retardance  $\delta$  in degrees vs. applied uniaxial compressive stress  $\bar{\sigma}$  in  $\text{kg/cm}^2$  for both "A" type samples and "B" type samples of KCl and KBr. The measurements were made at  $\lambda = 1.18$  microns. In all cases the maximum stress applied was within the linear stress-strain limit for each material. The total retardance includes retardation due to the compensator, the residual stress in the sample and the stress induced retardation. The stress optic coefficients  $C_{\lambda}$  and  $C'_{\lambda}$  from the data of Figure 1 is obtained from the slope of the curves as described in Appendix A. As can be seen from the results of Figure 1, the "A" samples have a positive slope, thus yielding a positive value for  $C_{\lambda}$  whereas the "B" samples yield a negative value for  $C'_{\lambda}$ .

Figure 2 shows results at  $\lambda = 5$  microns for KI "A" samples and KBr "B" samples in which the total retardance is plotted vs. stress.

\* Laser did not operate in a single  $\text{TM}_{00}$  mode but skipped rather frequently to other modes, thereby changing the beam spot configuration and hence, the spatial energy distribution, thus causing noise in the detector.

For these cases both values of the respective stress optic coefficients  $C_{\lambda}$  for KI and  $C'_{\lambda}$  for KBr are positive numbers. The total retardance vs. stress for are "A" and a "B" sample of LiF measured at 5 microns are given in Figure 3. It can be seen that for LiF at 5 microns both  $C_{\lambda}$  and  $C'_{\lambda}$  are negative. One additional comment for the results on LiF is that we are able to impress larger stress on the sample as compared with KBr and KCl since LiF has larger value of linear stress-strain response when compared to KCl and KBr.

We have found it was not possible to construct a retardance vs. stress curve for the case of NaCl at wavelengths longer than 8 microns because of the extremely low value of the stress birefringence response of this material in the linear stress-strain region. However, we can still obtain a value of  $C_{\lambda}$  and  $C'_{\lambda}$  for NaCl by using only two points, a procedure which is not as accurate as obtaining a slope based on a curve constructed from three or more points. Unfortunately this characteristic represents a limitation of our method as applied to some of the alkali halides.

One final series of retardance vs. stress curves measured at 5 microns for  $\text{CaF}_2$  "A" and "B" samples is given in Figure 4. Also, included in Figure 4 are similar results for  $\text{SrF}_2$ . It can be seen in the results of Figures 1-4 that well defined straight lines were obtained for all those materials which makes the extraction of the slope ( $C_{\lambda}$ , or  $C'_{\lambda}$ ) from the data relatively simple. Therefore, from such data we feel that our values of  $C_{\lambda}$  and  $C'_{\lambda}$  are uniquely determined and the experimental error relatively small ( $\lesssim 15\%$ ) in most cases.

The most significant and complete method of presenting the stress birefringence data is in the form of stress optic coefficient vs. wavelength. These data are given in Figure 5 for KCl and LiF for both "A" and "B" type samples which represent  $C_{\lambda}$  and  $C'_{\lambda}$  respectively. Our results include the wavelength range from  $\sim 1$  to 11 microns. Also shown in Figure 5 are stress optic coefficient results at  $\approx 0.6$  microns reported by Wilkening et.al.<sup>(4)</sup>, and Leibssle<sup>5</sup>. The rather strange behavior of the wavelength dependence of the stress optic coefficient for "B" type KCl samples (Figure 5) is puzzling. We have re-checked the experimental data and analysis of the measurements and are not able to find any errors, and hence must stand on

those results until further experiments are performed on KCl "B" type samples. In Figure 6 we show the experimental results for the wavelength dispersion of stress optic coefficient for KI and KBr "A" type ( $C_{\lambda}$ ) and "B" type ( $C'_{\lambda}$ ) samples. We have not yet made measurements on KI "B" near a wavelength of 1 micron. Note the dependence of the stress optic coefficient on wavelength for KBr "B" does not exhibit the strange behavior of KCl "B" shown in Figure 5. Included in the results of Figure 6 are the data of Wilkening et.al.<sup>(4)</sup> and Leibssle for stress optic coefficient measurements near 0.6 micron.

The inherently small stress birefringence exhibited by NaCl can be seen in the results of Figure 7. In fact the sign of the value at  $\sim 10.6$  micron for NaCl is in question. We were not able to make sufficiently accurate measurements near 10.6 microns to be able to definitively assign a positive or negative value. Further work is required for NaCl. In Figure 7 we also show some results for  $\text{CaF}_2$  "A" and "B" type samples and a measurement at 5 microns for "A" and "B" type samples of NaBr. Although the latter measurements are not complete they are included in this report to serve as an indication of the values of  $C_{\lambda}$  and  $C'_{\lambda}$  to be expected from these materials which previously were unknown. Data of Wilkening et.al.<sup>(4)</sup> and Leibssle<sup>(5)</sup> near 0.6 micron are also shown in Figure 7.

Further discussion of these results and comparisons with theory<sup>(2)</sup> will be made later after the presentation of stress optic properties of non-oxide glasses to be given next.

B. Non-oxide glasses ZnSe, ZnS,  $\text{SrF}_2$  and TI-1173 chalcogenide.

In general we have found the study of stress-optic response of the non-oxide glasses and other hard materials much easier to perform than the soft alkali halide materials. For the case of the hard materials one can use higher stress and obtain larger signals since basically the hard materials have stress optic coefficients whose values are about a factor 3 to 10 larger than the alkali halides. Some typical retardation vs. stress results for ZnS and ZnSe are given in Figure 8. The measurements were made at 5 microns. Note the relatively large total retardance for ZnS and ZnSe when compared to similar results in Figures 1 and 2 for the alkali halides KBr, KCl and KI. Finally, in Figure 9 we give the wavelength dependence of the stress optic coefficients of ZnSe, ZnS a chalcogenide glass TI-1173 and a few measure-

ments on  $\text{MgF}_2$  which were completed during the course of our program. A more complete wavelength dependence would require more additional effort, we include the limited number of measurements given in Figure 9 for purposes of indicating the stress optic properties of the non-oxide glasses previously not known.

It is important to discuss the sources of experimental error in results presented above (Figures 1-9). The major source of error for the alkali halides arises from the extremely small stress birefringence exhibited by these materials, especially in the linear stress-strain region, i.e., stress  $\lesssim 11\text{kg/cm}^2$ . The electronic signal to noise for the alkali halides must be small compared to typical stress birefringence signal values which are  $\sim 100 - 300 \text{ nV}$  or  $\sim 0.2\%$  full scale. This requires extreme stability of the electronics with respect to drift, pickup etc. We have minimized other sources of error, e.g., residual stress was minimized by annealing (to  $680^\circ\text{C}$  typically) polarizer angles were measured to better than  $0.5^\circ$ , and in general we made at least five measurements at each stress and wavelength value to determine reproducibility. Taking all the above factors into consideration we estimate our maximum error in  $C_\lambda$  and  $C_\lambda'$  for KCl, KI, KBr, and LiF to be  $\pm 15\%$  for  $\lambda > 3\mu$  and  $\pm 20\%$  at  $\lambda = 1.18\mu$ ; these large errors are due to the fact that the stress birefringence of NaCl is the smallest of all materials studied. In the case of the "hard" materials we estimate the errors to be  $\pm 12\%$  for ZnS, and  $\pm 10\%$  for ZnSe,  $\text{CaF}_2$ ,  $\text{MgF}_2$  and  $\text{SrF}_2$  over the wavelength region studied.

#### IV. Discussion of Results

##### A. Alkali Halides

Only one pertinent theoretical treatment which calculates stress birefringence vs. wavelength is presently available to make a comparison of our experimental results with theory; namely the work of Bendow and Gianino<sup>(2)</sup>. The comparison of theory with experiment cannot presently be made on the absolute values of  $C_\lambda$  and  $C_\lambda'$ , but rather we shall give a comparison of the values of the ratios of  $C_\lambda$  and  $C_\lambda'$  at several wavelengths with theory. In the case of NaCl it is not possible to make meaningful comparisons because of the large experimental uncertainty due to the very low value of  $C_\lambda$  and  $C_\lambda'$  exhibited by NaCl for  $\lambda > 2$  microns.

We have made our comparison of experiment with the theory of Bendow and Gianino<sup>(2)</sup> as follows: The elasto-optical coefficients  $p_{ij}$  are related to the stress optic constants by equations of the form,

$$p_{11} - p_{12} = (q_{11} - q_{12})(C_{11} - C_{12})$$

$$p_{44} = q_{44}C_{44}$$

where the  $C_{ij}$  are moduli of elasticity which are constants. Now since the  $q_{11} - q_{12}$  and  $q_{44}$  are directly proportional to  $C_\lambda$  and  $C_\lambda'$  respectively (apart from the constant  $\frac{n^3}{2}$  where  $n$  is the index of refraction) we have used the calculated values of  $p_{11} - p_{12}$  and  $p_{44}$  to compare with our measured values of  $C_\lambda$  and  $C_\lambda'$  at selected wavelengths. Specifically we have compared the ratios of  $C_\lambda$  and  $C_\lambda'$  at two wavelengths with the expected theoretical ratio. This comparison is tabulated below.

	$\lambda_1 = 1.18\mu$		$\lambda_2 = 5\mu$		$\lambda_3 = 11\mu$			
	$C_{\lambda_3}/C_{\lambda_1}$		$C_{\lambda_3}/C_{\lambda_2}$		$C'_{\lambda_3}/C'_{\lambda_1}$		$C'_{\lambda_3}/C'_{\lambda_2}$	
	Exp.	Theory	Exp.	Theory	Exp.	Theory	Exp.	Theory
KBr	1.75	2	1.18	1.66	0.58	1.43	0.91	1.32
KI	2.34	1.9	1.14	1.62	-	-	0.88	1.35
KCl	1.71	2.5	1	1.88	0.72	1.58	1.94	1.41

For the case of LiF the theory predicts a change of sign in  $q_{11} - q_{12}$  near  $5\mu$  which was not observed. In fact the calculated values for LiF show the greatest deviation from the measured values. We believe and have confidence that our LiF measurements are sufficiently accurate that

this deviation indicates to us that the theory and model may have serious deficiencies and should be re-examined. We have one more material where a good comparison with theory is possible. Namely, ZnS. At  $\lambda = 1.18\mu$  and  $\lambda_2 = 5\mu$  we obtain the following ratios of  $C_{\lambda_2}/C_{\lambda_1}$

Experiment	Theory
1.03	1.77

Although the experiments are not complete for the case of ZnSe, the measured  $C_{\lambda}$  values appear to have the wavelength dependence from 5 to 11 microns predicted by theory. It is not possible to make any further comparisons for the other materials studied thus far due to incompleteness of the data.

An examination of the above results of theory and experiment applied to KCl, KBr and KI indicates that the theory yields only an approximately correct wavelength dependence of  $C_{\lambda}$  and  $C_{\lambda}'$ , i.e., the theory is able to predict the wavelength dispersion of the stress optic coefficient well within a factor of two for most cases. Since our measurements represent the first reported data in this wavelength region it is somewhat premature to make a strong and definitive statement relative to the shortcomings of the theory. However, we believe we have a good deal of evidence which strongly suggests modifications of the theory are needed.

#### V. Conclusions and Recommendations

In this research program we have successfully extended the method of Michael<sup>(1)</sup> to measure the stress optic coefficients of materials at 296°K which transmit light in the 1 to 12 micron wavelength range. The materials studied include alkali halides and non-oxide glasses. Since some of the materials (NaCl, ZnS, and ZnSe) lack complete sets of stress optic properties vs. wavelength we recommend further measurements be made.

We have found that in general the "soft" alkali halide materials exhibit stress optic coefficients in the range  $\sim 1$  to 4 Brewsters which are factors of 3 to 10 smaller than what we observe for the "hard" non-oxide glasses in the wavelength region from 1 to 12 microns. The theory and model of Bendow and Gianino<sup>(2)</sup> although capable of predicting

the wavelength dispersion of the stress optic coefficients within a factor of  $\sim 2$  for most of the materials (except LiF) is in need of modification probably in the change of variable parameters used in the model.

The results to date suggest two additional directions should be taken in future work:

- a. Perform stress optic coefficient measurements from 12 to 20 microns, and
- b. Perform stress optic coefficient measurements at two additional temperatures, e.g., 78°K and  $\sim 400^\circ\text{K}$ .

The above research would be valuable in comparing to theory and model and additionally assisting in the formulation of theoretical models. We also strongly urge comparisons of measurements with other workers in this field who may be using different methods to obtain  $C_\lambda$  and  $C'_\lambda$ .

## ACKNOWLEDGMENT

We thank Dr. Carl Pitha and Dr. Lynn Skolnik of the United States Air Force Cambridge Laboratories, Bedford, Massachusetts, for informing us of the Michael method. We also thank Dr. Pitha for supplying us all the samples used in this study, and Dr. C. S. Chen of Burroughs Corporation for his invaluable assistance in the early phases of our program. Finally, we thank Dr. E. D. Palik of the U. S. Naval Research Laboratory for the use of his CdS and  $MgF_2$  Soleil compensators.

## References

1. A. J. Michael, J. Opt. Soc. Am. 58, 889 (1968).
2. B. A. Bendow and P. S. Gianino, "Calculations of the Frequency Dependence of Elasto-Optic Constants of Infrared Laser Window Materials", Air Force Cambridge Research Laboratories Report AFCRL-TR-74-0533, 24 October 1974, Hanscom AFB, Massachusetts 01730. This report contains references to earlier papers and reports on the theoretical aspects of the problem.
3. C. A. Pitha and J. D. Friedman, in Proc 4th Ann. Conf. on Infrared Laser Window Materials, 1974, p. 149. Conference held in Tucson, Arizona 18-20 November 1974.
4. W. W. Wilkening, J. Friedman, and C. A. Pitha, Third Conference on High Power Infrared Laser Window Materials, November 12-13, 1973, Vol I, AFCRL-TR-74-0085(1), pp. 353-366.
5. H. Leibssle, Zeit. fur. Kristall, Band 114, 457 (1960)

## FIGURE CAPTIONS

- Figure 1 Total retardance vs. applied stress for KBr and KCl "A" and "B" samples measured at  $\lambda = 1.18$  microns at  $296^\circ\text{K}$ .
- Figure 2 Total retardance vs. applied stress for a KI "A" sample and a KBr "B" sample measured at  $\lambda = 5$  microns at  $296^\circ\text{K}$ .
- Figure 3 Total retardance vs. applied stress for LiF "A" and "B" samples measure at  $\lambda = 5$  microns at  $296^\circ\text{K}$ .
- Figure 4 Total retardance vs. applied stress for  $\text{SrF}_2$  and  $\text{CaF}_2$  "A" and "B" samples measured at  $\lambda = 5$  microns at  $296^\circ\text{K}$ .
- Figure 5 Wavelength dependence of the stress optic coefficient of "A" and "B" samples of KCl and LiF at  $296^\circ\text{K}$ .
- Figure 6 Wavelength dependence of the stress optic coefficient of "A" and "B" samples of KI and KBr at  $296^\circ\text{K}$ .
- Figure 7 Wavelength dependence of the stress optic coefficient of "A" and "B" samples of NaCl,  $\text{CaF}_2$  at  $296^\circ\text{K}$ . Also shown is a measurement of NaBr "A" and "B" samples at  $\lambda = 5$  microns.
- Figure 8 Total retardance vs. applied stress for ZnS and ZnSe at  $\lambda = 5$  microns at  $296^\circ\text{K}$ .
- Figure 9 Wavelength dependence of the stress optic coefficient of ZnSe, ZnS,  $\text{MgF}_2$  ("A" sample) and TI-1173 chalcogenide glass at  $296^\circ\text{K}$ .

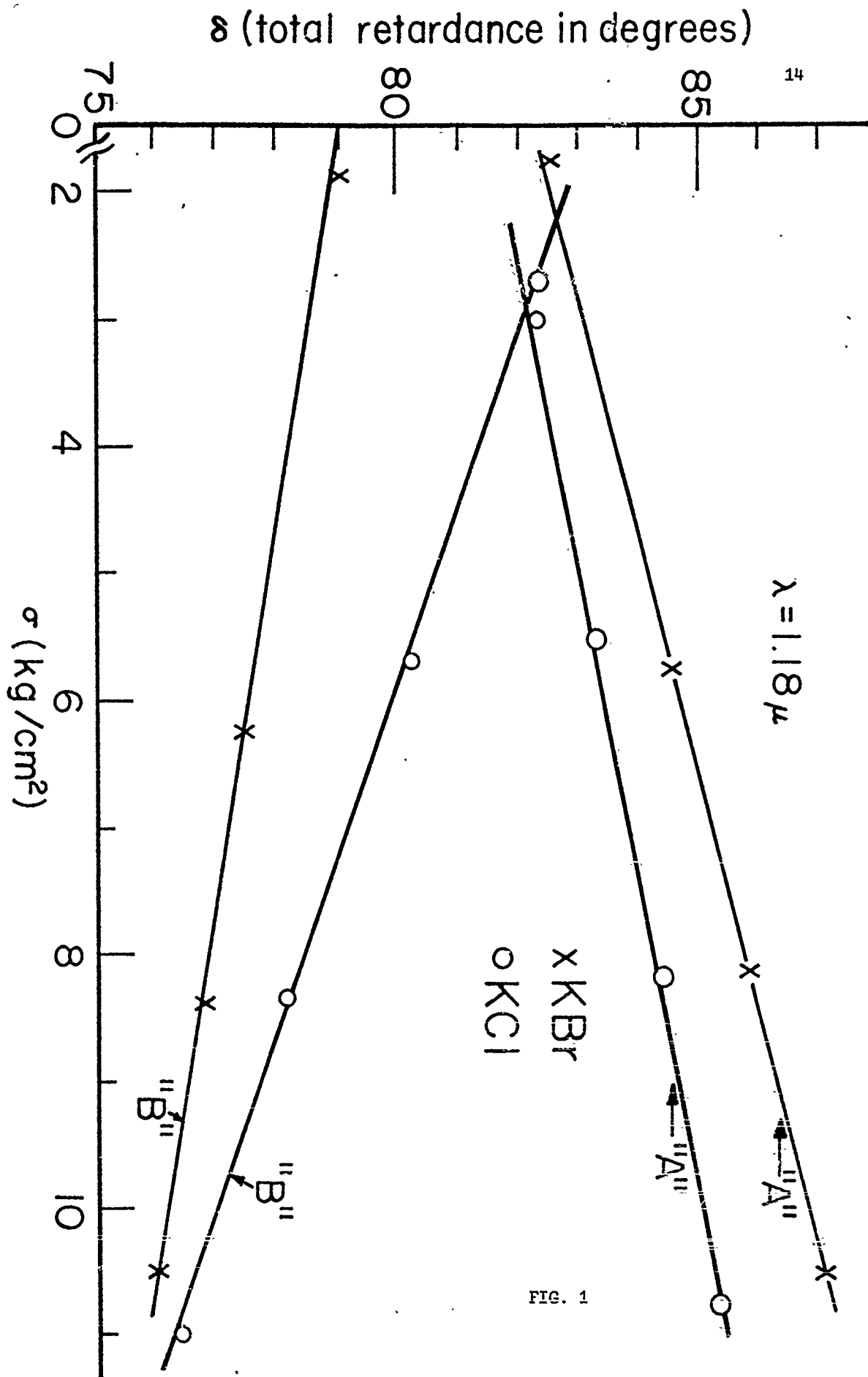


FIG. 1

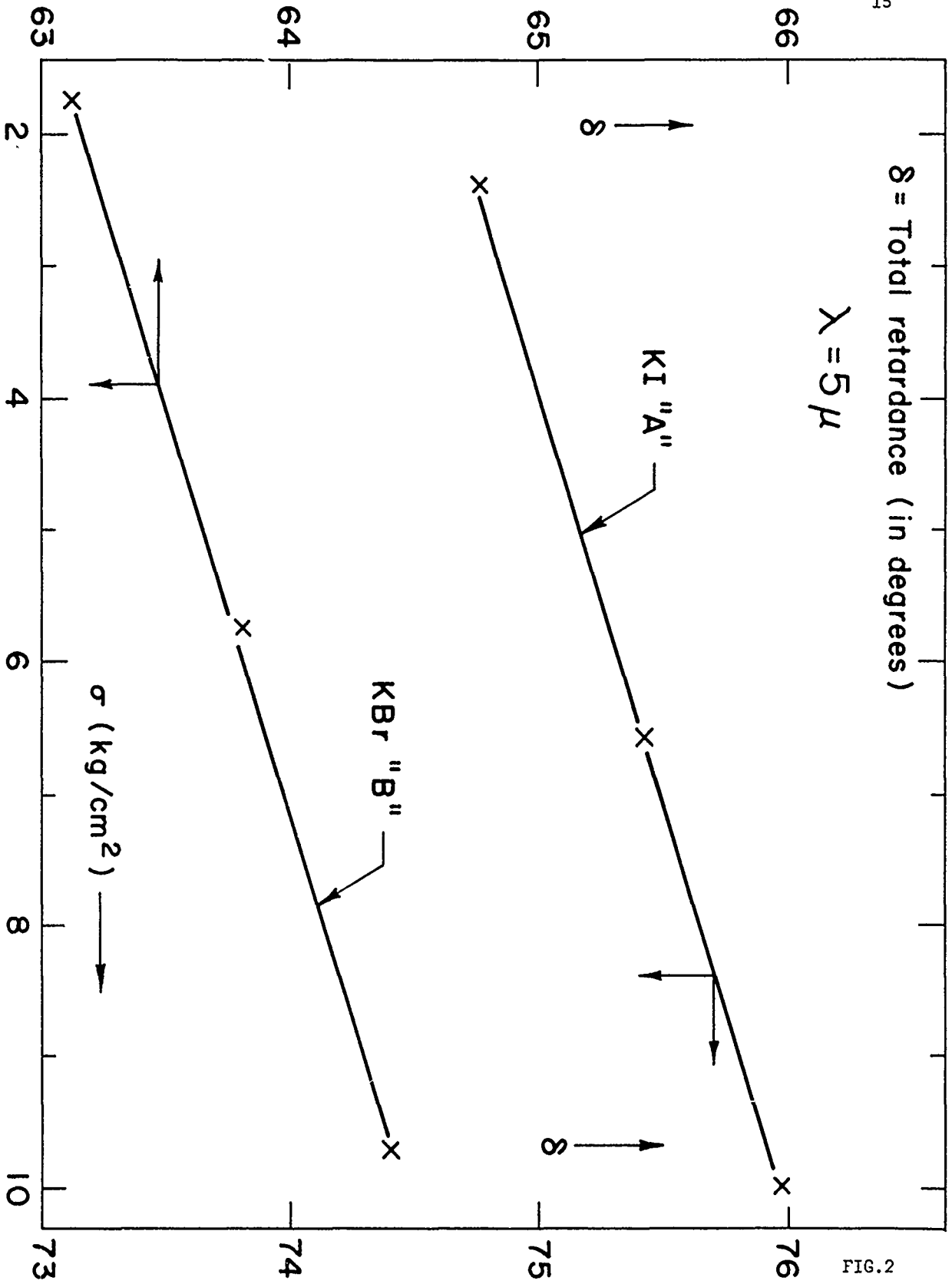
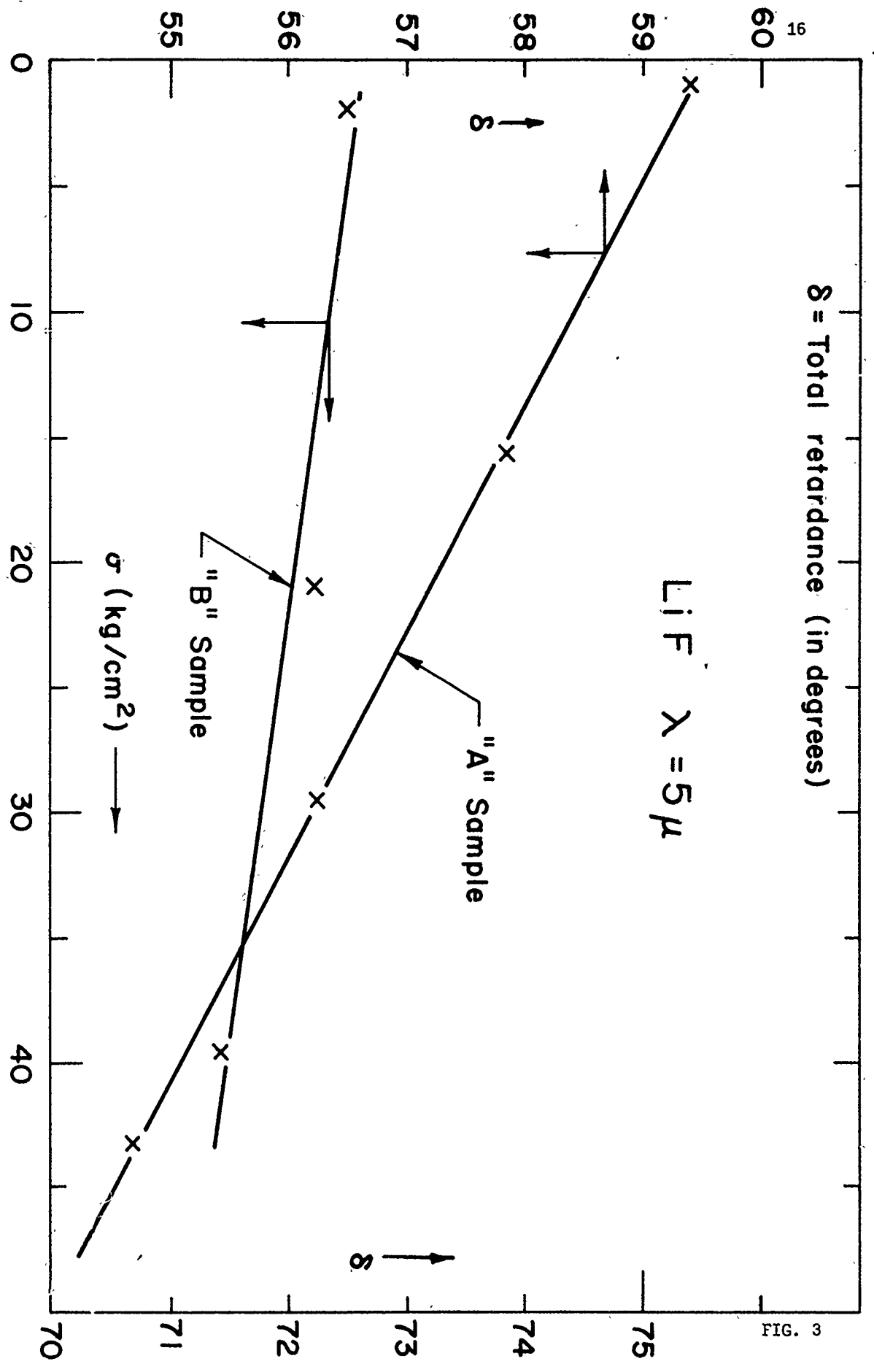


FIG. 2



$\delta$  = Total retardance (in degrees)

LIF  $\lambda = 5 \mu$

"A" Sample

"B" Sample

$\sigma$  (kg/cm<sup>2</sup>)

FIG. 3

$\lambda = 5\mu$

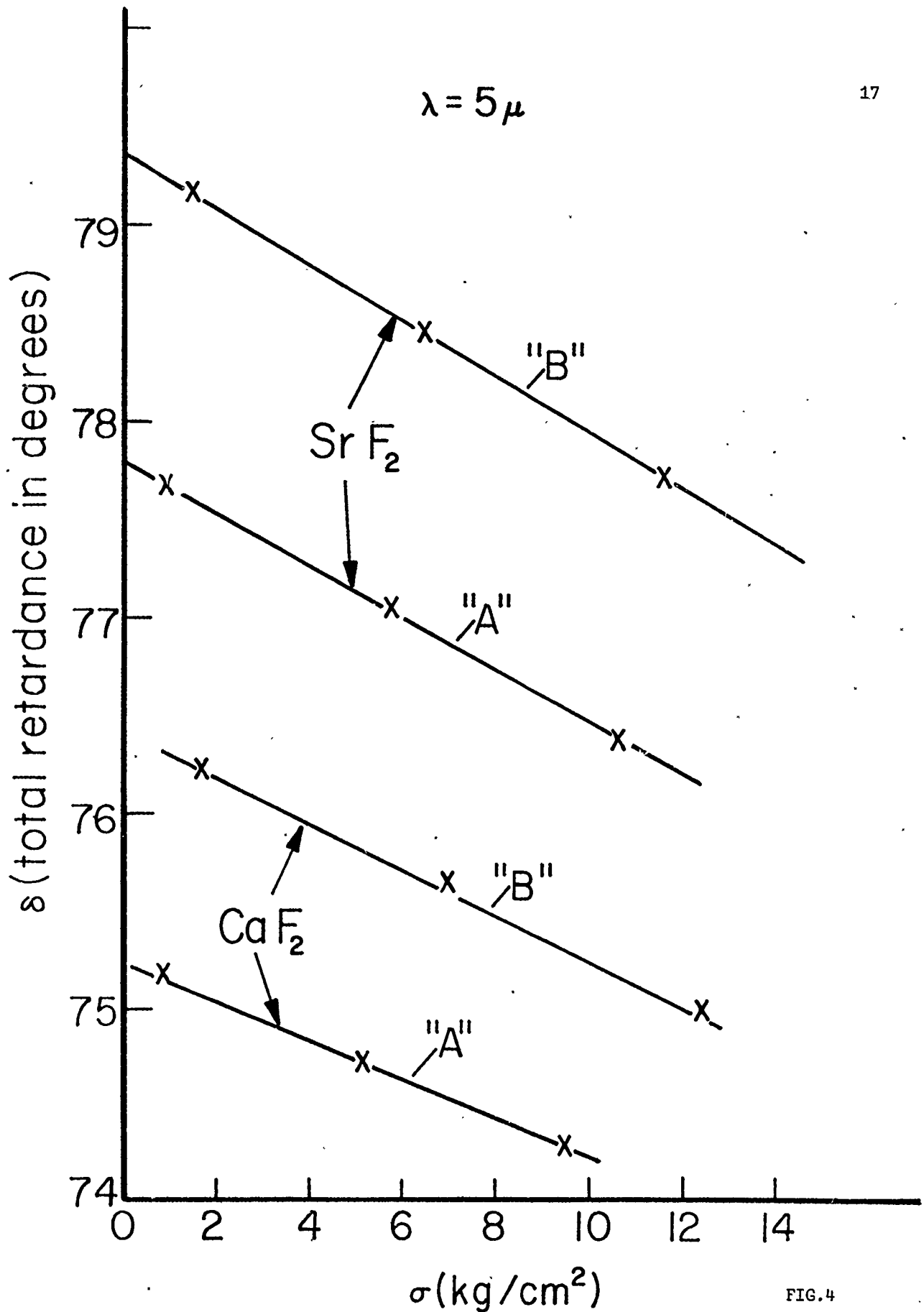


FIG. 4

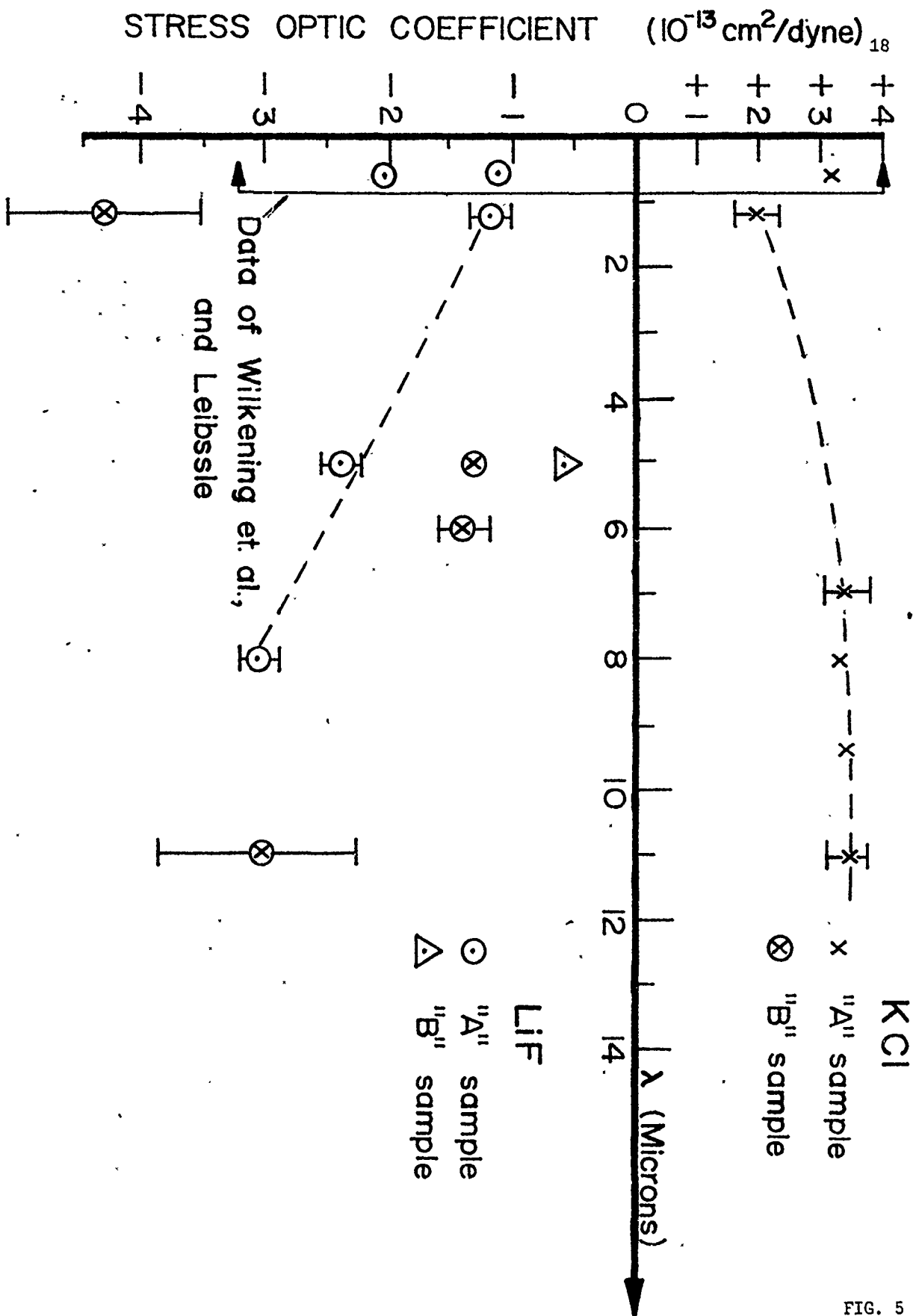


FIG. 5

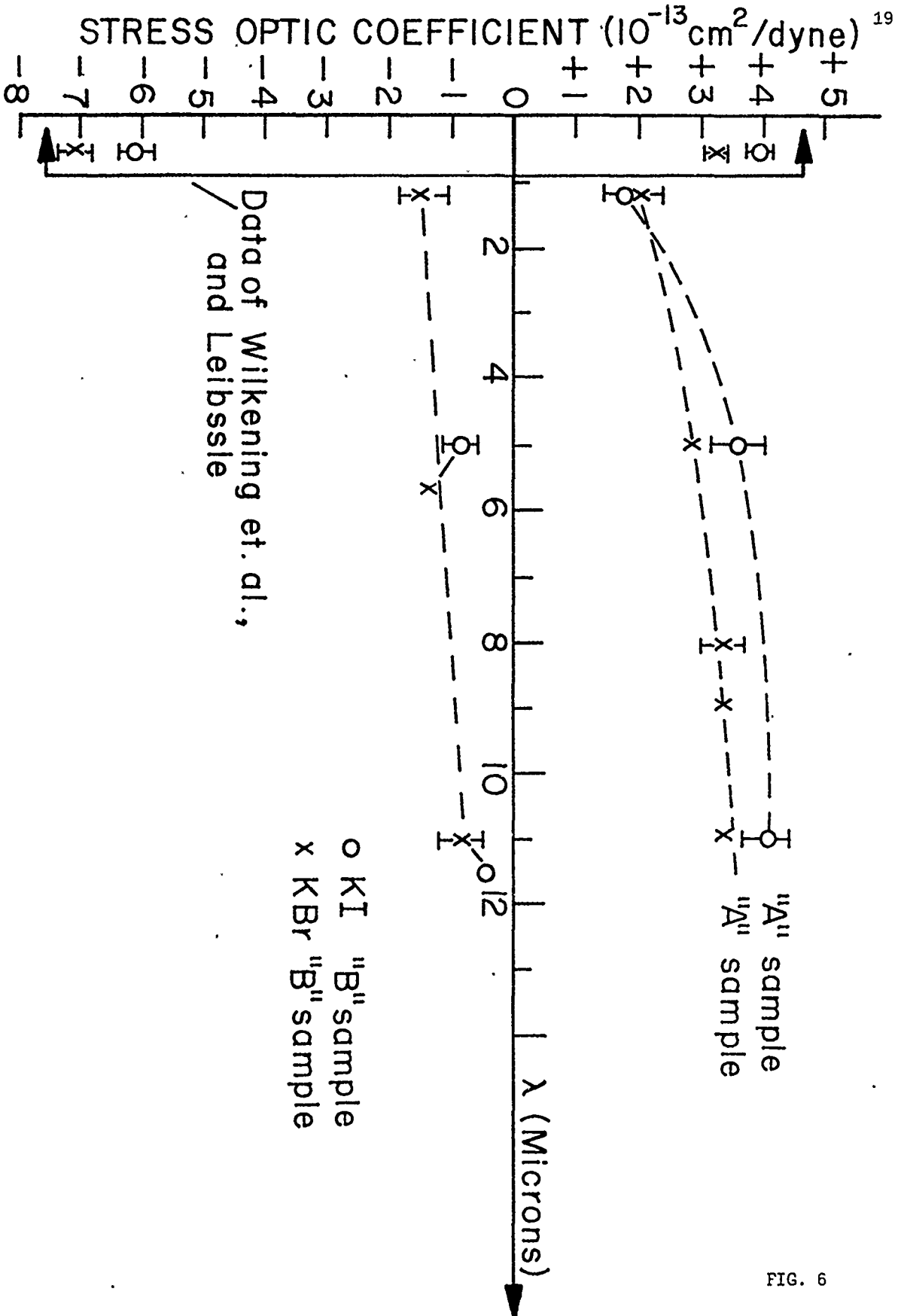


FIG. 6

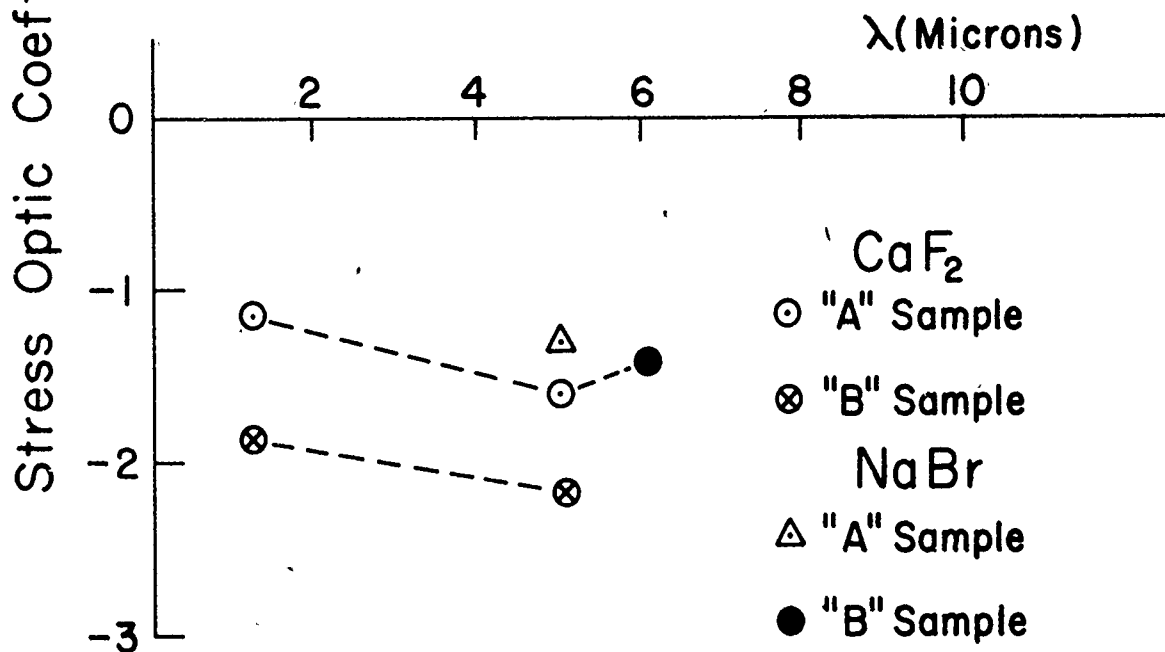
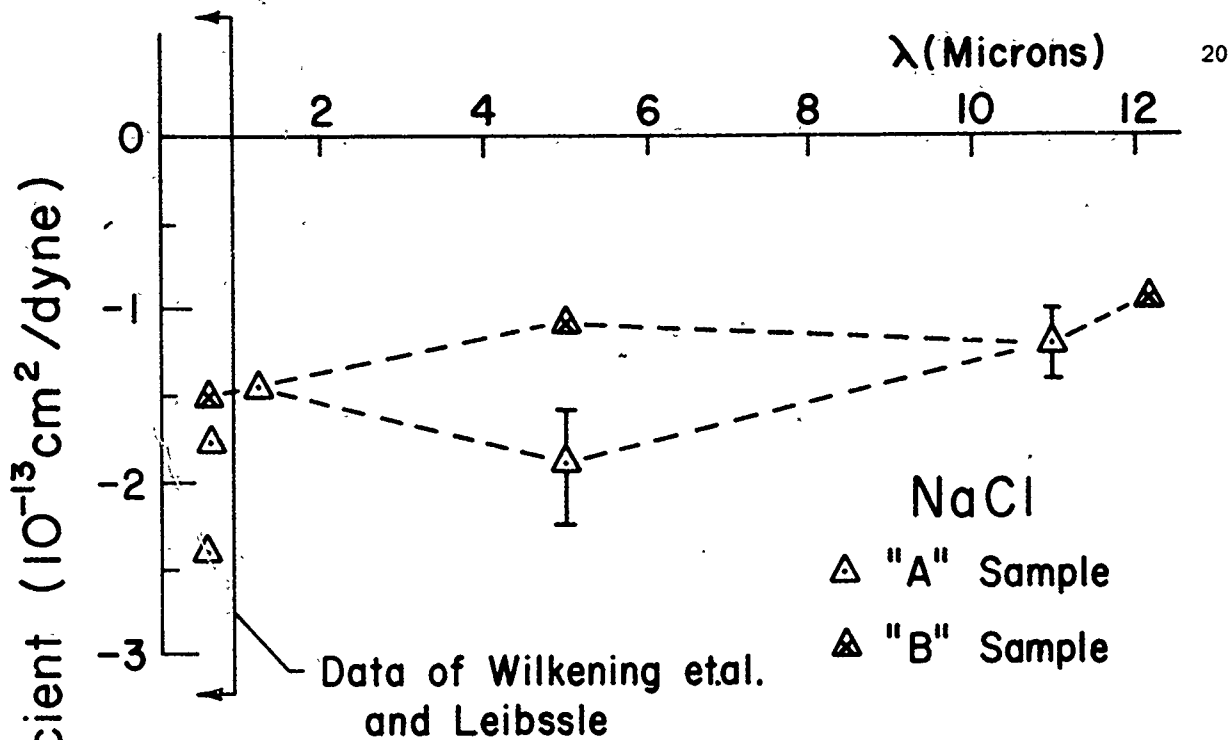
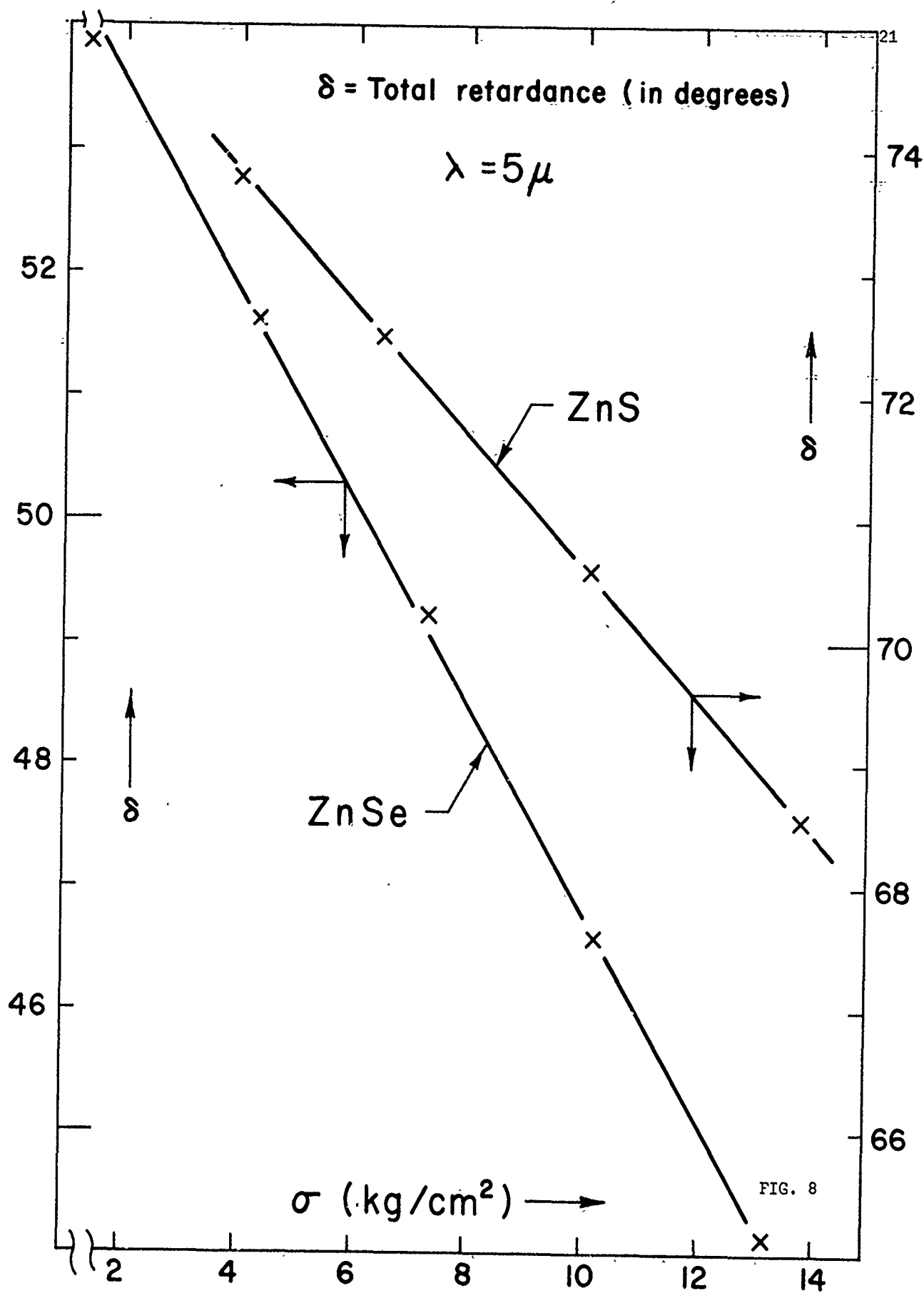


FIG. 7



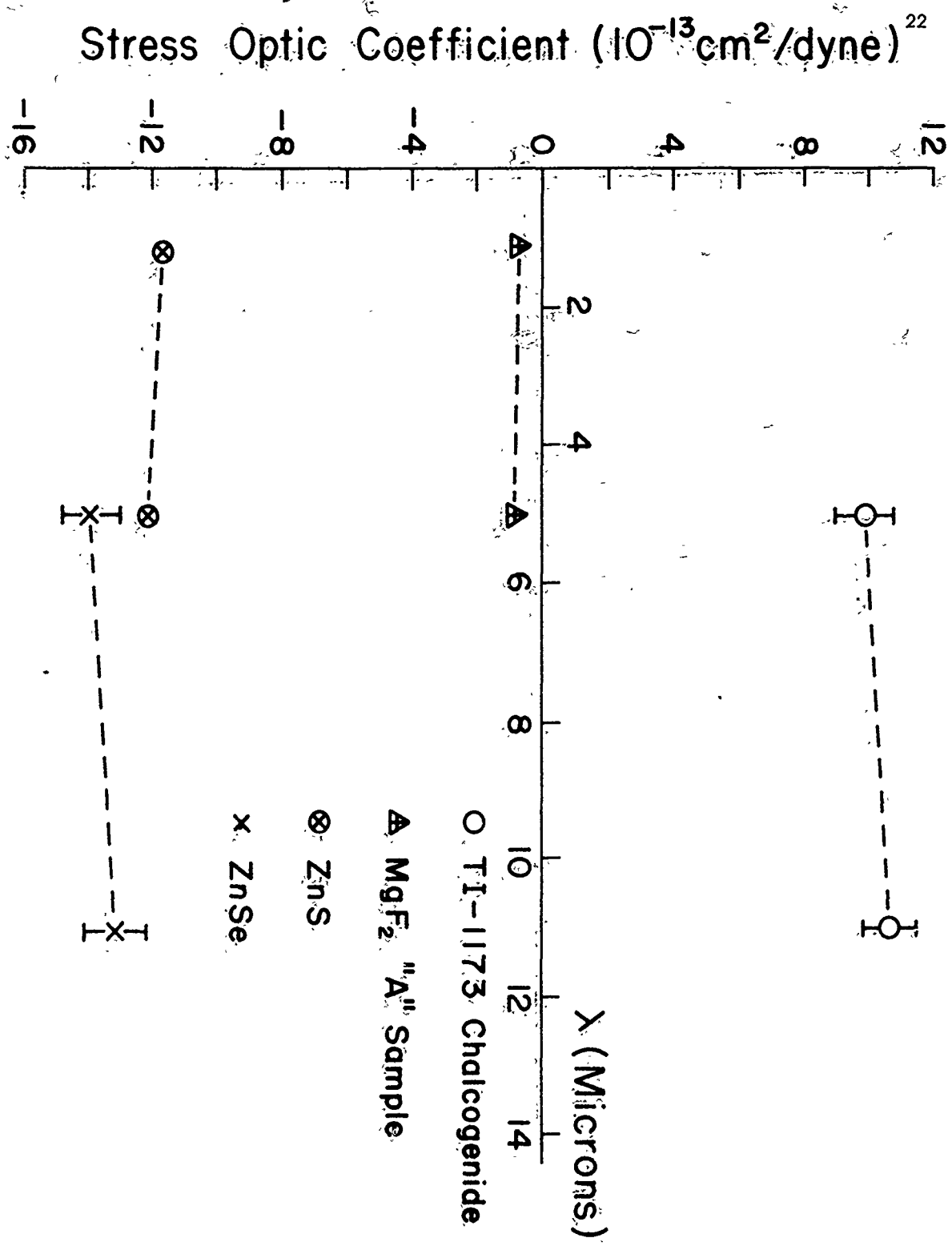


FIG. 9

## Infrared stress birefringence in KBr, KCl, LiF, and ZnSe<sup>†</sup>

C. S. Chen\*, J. P. Szczesniak, and J. C. Corelli<sup>†</sup>

*Division of Nuclear Engineering, Rensselaer Polytechnic Institute, Troy, New York 12181*  
(Received 1 July 1974)

The application of a variation of intensity method using static stress and polarized light to measure stress birefringence in the infrared wavelength region ( $\sim 4\text{--}11\ \mu\text{m}$ ) is described. We have used this method to measure the stress optic coefficient  $C_\lambda$  for the alkali halide cubic crystals KBr, KCl, LiF, and polycrystalline ZnSe. A detailed discussion of the definition of  $C_\lambda$  in terms of piezo-optic coefficients is given in the paper. Our results indicate that no wavelength dependence is observed for  $C_\lambda$  in the  $4\text{--}11\text{-}\mu\text{m}$  region for KCl and KBr which have typical measured  $C_\lambda$  values of  $+3.3$  and  $+3.4$  Brewsters, respectively. For LiF at  $8\ \mu\text{m}$  we get  $C_\lambda = -3.08$  Brewsters and for ZnSe we obtain  $C_\lambda$  values of  $-13.2$  Brewsters at  $9.4\ \mu\text{m}$  and  $-13.0$  Brewsters at  $11\ \mu\text{m}$ .

### I. INTRODUCTION

In recent years high-power ( $> 5\ \text{kW}$ )  $\text{CO}_2$  lasers have become readily available and are used in a wide variety of applications. When such high-power lasers are used in conjunction with window material/the light beam at  $10.6\ \mu\text{m}$  can become distorted in penetrating the window due to local thermal stress effects. Thus, one must understand and carefully characterize the relevant parameters which enter in the distortion process of the solid window material.

In this paper we approach one aspect of the problem for study, namely, the measurement of the stress optic properties (at  $300\ \text{K}$ ) of some alkali halide salts (KCl, KBr, and LiF) and a nonoxide glass (ZnSe). Specifically, our experiments were designed to measure stress optic response of the materials just mentioned in the linear stress-strain region and in the infrared wavelength range of  $4\text{--}12\ \mu\text{m}$ , with particular attention for wavelengths near the  $10.6\text{-}\mu\text{m}$   $\text{CO}_2$  laser line.

A search of the literature reveals that the dispersion of the stress optic coefficient  $C_\lambda$  has been measured for some alkali halide crystals only in the visible<sup>1-4</sup> and ultraviolet<sup>5,6</sup> wavelength region. We shall define  $C_\lambda$  in what follows. Others have reported measurements on stress birefringence in Ge,<sup>7</sup>  $\text{SrTiO}_3$ ,<sup>8</sup> GaAs,<sup>9</sup> ruby,<sup>10</sup> and various glasses<sup>11,12</sup>; in all cases the previous measurements of stress-induced birefringence were obtained only for light having wavelengths  $\lambda \lesssim 2\ \mu\text{m}$ .

We have extended the intensity crossed-polarizer method of measuring the stress-induced retardance reported by Michael<sup>13</sup> to determine the stress optic coefficient of solids in the infrared region  $4\text{--}12\ \mu\text{m}$ . As will be seen, we do not observe any changes in the stress optic coefficient  $C_\lambda$  of KCl, and KBr in the  $6\text{--}12\text{-}\mu\text{m}$  wavelength region. Previous investigations<sup>1-4</sup> indicate that large variations of  $C_\lambda$  with  $\lambda$  for alkali halides occur in the vicinity of the fundamental absorption bands near the ultraviolet light wavelength region. However, the dispersion of  $C_\lambda$  for alkali halides in the visible region is small,  $\approx 5\text{--}10\%$ .

In this paper we shall give first a detailed discussion of the method for intensity calculations as they apply to Michael's method of measuring  $C_\lambda$ ; we shall describe how we perform the measurement in the  $4\text{--}12\text{-}\mu\text{m}$  wavelength region; finally we shall present stress-birefringence results on KCl, KBr, LiF, and ZnSe.

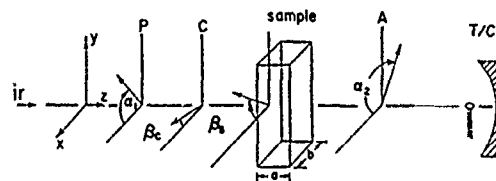
### II. THEORY OF MEASUREMENT

#### A. Intensity calculation

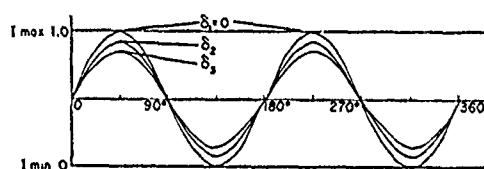
It was first pointed out by Mueller<sup>14</sup> on the basis of a paper by Soleillet<sup>15</sup> that the Stokes parameters which describe a general beam of light could be regarded as the components of a column matrix of a 4-vector. Thus, we can represent a beam of elliptically polarized light by the 4-vector

$$\begin{aligned} I &= \langle E_x^2 + E_y^2 \rangle, \\ Q &= \langle E_x^2 - E_y^2 \rangle, \\ U &= \langle 2E_x E_y \cos \delta_0 \rangle, \\ V &= \langle 2E_x E_y \sin \delta_0 \rangle, \end{aligned} \quad (1)$$

where  $E_x$  and  $E_y$  are the instantaneous positive values of the components of the electric field vector in a rectangular coordinate system in which the beam is propagating in the  $z$  direction, and  $\delta_0$  is the instantaneous relative phase difference restricted to values between  $-\pi$  and  $+\pi$ . The angular brackets in Eqs. (1) represent the time averages. The action of any optical device on



(a)



(b)

FIG. 1. (a) Coordinate system and optical arrangement of stress optic coefficient measurement, infrared light  $I_r$  incident in  $z$  direction. P, polarizer; C, CdS compensator; A, analyzer, T/C, thermocouple detector. (See text for discussion of angles  $\alpha_1$ ,  $\beta_c$ ,  $\beta_1$ , and  $\alpha_2$ .) (b) Sinusoidal variation of intensity as a function of analyzer-angle  $\alpha_2$  for various retardances  $\delta_1$  ( $\delta_1 < \delta_2 < \delta_3$ ).

the beam such as a polarizer, quarter-wave plate, etc., is to transform the polarization of the beam from one state to another. Therefore, any optical device which changes the state of polarization of a beam may be represented by a  $4 \times 4$  matrix and any series of such optical devices can be represented by the direct product of their individual  $4 \times 4$  matrices.

We have modified and extended the method of Michael<sup>13</sup> for measuring stress birefringence to apply to the infrared region  $3-12 \mu\text{m}$ . Monochromatic light is supplied by a NaCl monochromator prism system. This monochromatic light enters the optical system which is the essential feature of our method for measurement and is shown schematically in Fig. 1(a). Our system consists of a wire grid polarizer and analyzer, a CdS Soleil compensator,<sup>16</sup> sample in a stress apparatus, and a thermocouple detector. As a compressive uniaxial stress is impressed on the sample it becomes birefringent and the stressed sample acts like a retarder. Thus, the stressed sample is effectively another optical device which can alter the light beam polarization. The angles  $\alpha_1$  and  $\alpha_2$  are the azimuth angles of the polarizer and analyzer, respectively, and are measured with respect to the horizontal  $x$  axis which is taken as the zero azimuth [see Fig. 1(a)]. The angles  $\beta_c$  and  $\beta_s$  are the azimuth angle of the fast eigenvector of the CdS compensator and retarder (stressed sample), respectively, with respect to the  $x$  axis, and  $\delta_c$  and  $\delta_s$  are the retardance of the compensator and sample, respectively.

We stated earlier that each optical device which changes the state of polarization may be represented by a  $4 \times 4$  matrix and the transmitted light intensity after

passing through a series of such optical devices can be obtained by routine calculation of the matrix products as shown in Eq. (2):

$$A = [P(\alpha_2)R(\beta_s, \delta_s)R(\beta_c, \delta_c)P(\alpha_1)P_p(x)] \begin{bmatrix} E_x^2 + E_y^2 \\ E_x^2 - E_y^2 \\ 2E_x E_y \cos \delta_0 \\ 2E_x E_y \sin \delta_0 \end{bmatrix} \quad (2)$$

The matrix of a partial polarizer which produces a degree of polarization  $P_x$  and  $P_y$  in the  $x$  and  $y$  directions, respectively, is obtained by Billings and Land<sup>17</sup> as

$$P_p = \frac{1}{2} \begin{bmatrix} P_x^2 + P_y^2 & P_x^2 - P_y^2 & 0 & 0 \\ P_x^2 + P_y^2 & P_x^2 + P_y^2 & 0 & 0 \\ 0 & 0 & 2P_x P_y & 0 \\ 0 & 0 & 0 & 2P_x P_y \end{bmatrix} \quad (3)$$

According to Walker,<sup>18</sup> the matrix of a polarizer  $P(\alpha)$  which produces perfect polarization along a line at an angle  $\alpha$  with respect to the  $x$  axis, and a plate of retardation  $\delta$  with an angle  $\beta$  with respect to the  $x$  axis can be written as

$$P(\alpha) = \frac{1}{2} \begin{bmatrix} 1 & \cos 2\alpha & \sin 2\alpha & 0 \\ \cos 2\alpha & \cos^2 2\alpha & \sin 2\alpha \cos 2\alpha & 0 \\ \sin 2\alpha & \sin 2\alpha \cos 2\alpha & \sin^2 2\alpha & 0 \\ 0 & 0 & 0 & 0 \end{bmatrix} \quad (4)$$

and

$$R(\beta, \delta) = \begin{bmatrix} 1 & 0 & 0 & 0 \\ 0 & \cos^2 2\beta + \sin^2 2\beta \cos \delta & \cos 2\beta \sin 2\beta (1 - \cos \delta) & \sin 2\beta \sin \delta \\ 0 & \sin 2\beta \cos 2\beta (1 - \cos \delta) & \sin^2 2\beta + \cos^2 2\beta \cos \delta & -\cos 2\beta \sin \delta \\ 0 & -\sin 2\beta \sin \delta & \cos 2\beta \sin \delta & \cos \delta \end{bmatrix} \quad (5)$$

The resulting matrix of Eq. (2) becomes very complicated even if we compute only the first element of the column, the intensity, which is of prime interest to us. However, as is the case for a perfect polarizer ( $P_x = 1, P_y = 0$ ), if the azimuth angle  $\alpha_1$  of the polarizer is set at  $\pm 45^\circ$  and  $\beta_c = \beta_s = 0$  the intensity of transmitted light  $I$ , which is the first element of the column, assumes a very simple form, i. e.,

$$I = \frac{1}{2} E_x^2 [1 + \cos(\delta_c + \delta_s) \sin 2\alpha_2], \quad (6)$$

or

$$I^1 = I/E_x^2 = \frac{1}{2} (1 + \cos \delta \sin 2\alpha_2), \quad (7)$$

where

$$\delta = \delta_c + \delta_s.$$

As shown by Michael<sup>13</sup> if we plot  $I^1$  vs the azimuth angle  $\alpha_2$  for different retardances  $\delta$  we get a periodic variation of intensity with  $\delta$  and  $\alpha_2$  [see Fig. 1(b)].

In Fig. 1(b) we see that the maximum change of the normalized intensity  $I^1$  due to the retardance  $\delta$  occurs at  $\alpha_2 = 45^\circ + n\pi$  or  $\alpha_2 = 135^\circ + n\pi$  ( $n = 0, 1, 2, \dots$ ). For those angles  $\alpha_2$  where the intensity is a maximum or a minimum the retardance can be easily determined by measuring the intensity  $I_{\text{max}}(\alpha_2 = 45^\circ)$  and  $I_{\text{min}}(\alpha_2 = 135^\circ)$ :

$$I_{\text{max}} = \frac{1}{2}(1 + \cos \delta), \quad I_{\text{min}} = \frac{1}{2}(1 - \cos \delta); \quad (8)$$

recalling that  $I_{\text{max}} + I_{\text{min}} = 1$  for normalization we can rewrite Eq. (8) as

$$\cos \delta = \frac{I_{\text{max}} - I_{\text{min}}}{I_{\text{max}} + I_{\text{min}}} = I_{\text{max}} - I_{\text{min}}. \quad (9)$$

The intensity method reported by Michael<sup>13</sup> which does not utilize a compensator in front of the sample is applicable only in the wavelength region where the retardance is sufficiently large that the change of transmitted light intensity is measurable, a situation which

applies to the visible and uv wavelength regions. However, in the infrared wavelength region, as one might expect from measurements in the visible region,<sup>1-6</sup> the stress-induced retardance is small ( $\delta_s < 3^\circ$ ) and the corresponding intensity change is not easily measurable. The addition of a known retardance  $\delta_c$  in the form of a compensator placed in the optical path as in Fig. 1(a) will now add to the  $\delta_s$  and result in a very large increase in intensity differences by a factor  $\sim 20$ . This increase in intensity difference results from the fact that the intensity has a  $\cos^2\delta$  dependence [see Eqs. (7) and (8)] with maximum change in  $I^1$  occurring for  $\delta$  near  $45^\circ$ .

### B. Stress optic coefficient $C_\lambda$ , stress birefringence

Stress birefringence or stress-induced double refraction arises from the change in refractive index with different direction in the isotropic material when a compressive uniaxial stress is applied to cubic crystals such as KCl, KBr, etc. The change in index of refraction thus can be described in terms of a dimensionless quantity  $\Delta K_{ij}$ , the components of the dielectric tensor, or  $\Delta B_{ij}$ , the components of the relative dielectric impermeability tensor. Since the change of refractive index  $\Delta n_{ij} = (\Delta K_{ij})^{1/2} = (\Delta B_{ij})^{1/2}$  we can write

$$\Delta B_{ij} = q_{ijkl} \sigma_{kl}, \quad (10)$$

where the  $q_{ijkl}$  are the stress optical or piezo-optic constants and have units of Brewsters (1 Brewster =  $10^{-13}$  cm<sup>2</sup>/dyn) and  $\Delta B_{ij}$  is the change in birefringence  $B_{ij}$  caused by the stress  $\sigma_{kl}$  (in dyn/cm<sup>2</sup>). Equation (10) can be rewritten as

$$\Delta B_{ij} = P_{ijkl} \epsilon_{kl}, \quad (11)$$

where the  $P_{ijkl}$  are the elasto-optical coefficients (or strain optical constants) and  $\epsilon_{kl}$  are the elastic strain tensor components. Finally one can relate the  $p$ 's and  $q$ 's by

$$P_{ijrs} = q_{ijkl} C_{klrs} \quad \text{or} \quad q_{ijkl} = P_{ijrs} S_{rskl}, \quad (12)$$

where the  $S_{rskl}$  are the elastic compliance constants and the  $C_{klrs}$  are the elastic stiffness constants or moduli of elasticity. One can obtain the magnitude of stress-induced birefringence of a crystal by passing linearly polarized light through the crystal and analyzing the emerging light through a second polarizer (the analyzer) and in this way obtain the relative retardance induced by the stress.

For a cubic crystal with light incident in a [100] direction and stressed in a [010] direction the stress optic coefficient or the birefringence  $C_\lambda$  can be obtained from the photoelastic stress tensor with the result

$$C_\lambda = \frac{1}{2} n_0^3 (q_{11} - q_{12}), \quad (13)$$

where  $n_0$  is the index of refraction and the  $q_{11}$ ,  $q_{12}$  are particular stress tensor components of the piezo-optic constants. On the other hand, if now the cubic crystal is stressed in a [110] direction and light passes through the crystal in a [001] direction, then  $C_\lambda$  becomes

$$C_\lambda = \frac{1}{2} n_0^3 q_{44} \quad (14)$$

and the  $q_{44}$  is also a particular stress tensor component of the piezo-optic constant. In this paper we shall re-

port only  $C_\lambda$  measurements defined as in Eq. (13).

Consequently we see that the salient feature of the Michael<sup>13</sup> method is that by measuring the relative phase retardation caused by the stress we can obtain  $q_{11} - q_{12}$ , and/or  $q_{44}$  and thus  $C_\lambda$ .

### III. EXPERIMENTAL METHODS

The experimental arrangement for measuring  $C_\lambda$  in the wavelength region 3 to 12  $\mu$ m is shown schematically in Fig. 2. A Perkin-Elmer model 98 monochromator using a NaCl prism supplies monochromatic light to the sample. The light beam is chopped at 13 Hz by a Princeton Applied Research (PAR) Corp. model 222 chopper which also supplies a reference signal to the PAR model HR-8 phase-sensitive lock-in amplifier. The thermocouple detector signal is first amplified in a PAR model 90 preamplifier, then fed to the HR-8 amplifier. The amplifier output signal is recorded on a Varian model G-4000 recorder.

The sample-stressing apparatus consists of 1  $\frac{1}{4}$ -in. o.d. 1-in. i.d. stainless steel tube with a 1-in. solid stainless steel plunger that has a smooth sliding fit inside the hollow stainless steel tube. The sample is located in the hollow tube where there are light inlet and outlet apertures between a bottom stop and the plunger. A hydraulic jack with 1-ton capacity having a  $\frac{3}{4}$ -in. diam piston and 1-in. travel is used to exert a force between the 1-in. diam plunger and the hollow tube. A W.C. Dillion Co. force gauge (compression model 100-lb capacity) accurate to  $\pm 0.2$  lb is inserted between the hydraulic piston and the solid plunger to measure the force applied on the sample. To ensure uniform stress on the sample its ends are polished parallel and thin sheets of indium metal are placed between each end of the sample and the flat bearing surfaces of the plunger and the bottom stop at the end of the tube.

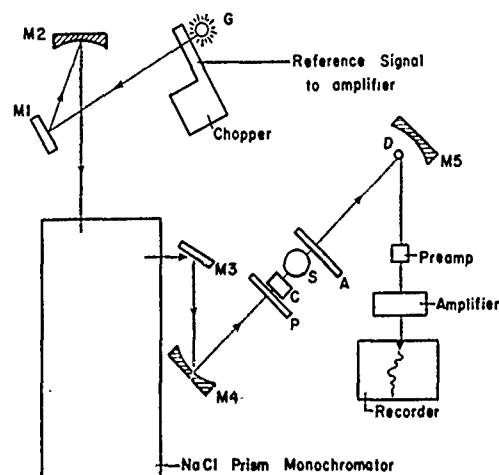


FIG. 2. Schematic of apparatus for measuring stress optic coefficients,  $C_\lambda$  vs  $\lambda$ .  $M_1$ - $M_5$ , front surface mirrors; P, wire grid polarizer; A, wire grid analyzer; C, CdS Soleil compensator; S, sample in stresser; D, thermocouple detector; G, global light source.

### A. Sample preparation

Rectangular bar samples<sup>19</sup> having nominal dimensions  $8 \times 9 \times 19$  mm are used. The KCl, KBr, and LiF samples were oriented with the long dimension in a [100] direction. Before any heat treatment most of the alkali halide samples exhibit a large amount of residual ingrown stress with their eigenvectors pointing along the [110] slip plane directions. It is evident that the eigenvectors of the residual stress do not coincide with the fast eigenvector of retardance induced by stress. Utilizing the mathematics of our intensity calculation we should be able to obtain the expression for the intensity with the optical path containing several retarders as long as the relative angles between their eigenvectors are known. However, the expression for the intensity reduces to a very simple form [Eq. (7)] if we select for measurement only those samples (KCl, KBr, and LiF) which have residual stress with their eigenvectors coinciding with the stress direction or select those samples with very small residual stress as manifested by retardance angles  $\lesssim 2^\circ$ .

The alkali halide samples were all given a heat treatment to within  $\sim 40^\circ\text{C}$  of their melting temperature for 10–20 h in a dry nitrogen gas atmosphere, followed by slow cooling at a rate of  $20^\circ\text{C/h}$ . Such a heat treatment reduces the residual stress to the condition which gives only  $\sim 2^\circ$  of relative retardance. Only samples having a residual stress relative retardance of  $\sim 2^\circ$  were selected for the stress optic coefficient measurements.

### B. Determination of $C_\lambda$ from the data

We give here a detailed description of how we apply Michael's method<sup>13</sup> and extend it to the  $4\text{--}12\text{-}\mu\text{m}$  wavelength region to obtain values of  $C_\lambda$  from the data. An over-all schematic of the apparatus used to measure  $C_\lambda$  versus  $\lambda$  is given in Fig. 2. It is important to note that it is very difficult to measure the stress-induced retardation angle  $\delta$  for the alkali halides above  $7\ \mu\text{m}$  because of very low signals. We shall point out the critical aspects where signal-to-noise considerations enter. In order to make the measurements with minimum experimental error ( $\sim 5\%$ ) it is important to eliminate or greatly reduce all possible errors which might occur due to imperfections in the polarizers, the compensator, angular alignment, and different source intensities at different wavelengths ( $3\text{--}12\ \mu\text{m}$ ). To accomplish this end we have developed a special way of normalization to obtain  $C_\lambda$  from the experimental data.

If we normalize  $I_{\text{max}} + I_{\text{min}}$  as 1.00 then we can rewrite Eq. (9) as

$$\cos\delta = 1 - (\Delta_1 + \Delta_2), \quad (15)$$

where  $\Delta_1$  and  $\Delta_2$  are the changes in intensity due to  $\delta$  (the retardance) at  $45^\circ$  and  $135^\circ$  azimuth angles, respectively [see Fig. 3(a)]. For the ideal case of perfect polarizers and compensator  $\Delta_1 = \Delta_2 = \Delta$  and  $\cos\delta = 1 - 2\Delta$ . However, in our experiments  $\Delta_1$  and  $\Delta_2$  are not equal and can differ by 2–5%, which we attribute to slight imperfections in the polarizers and compensator. We shall apply Eq. (9) and (10) to our typical experimental measurements on a step-by-step basis to show how we finally obtain  $C_\lambda$  and  $\delta$ .

First, the polarizer is set for  $\alpha_1 = 45^\circ$  and kept there for all subsequent measurements and the monochromator is set to give a monochromatic beam at some wavelength  $\lambda = \lambda_1$  in the  $4\text{--}12\text{-}\mu\text{m}$  range, there is no sample and no retardation (compensator set for  $0^\circ$  retardation) in the beam [see Fig. 1(a)]. We obtain for the measured transmitted intensities on the recorder chart in this case the typical values  $I_{\text{max}}^0(\alpha_2 = 45^\circ) \cong 97\%$ , and  $I_{\text{min}}^0(\alpha_2 = 135^\circ) \cong 1\%$  [see Fig. 3(b)]. In the second step we add a fixed retardation  $\delta_c$  (typically  $\approx 50^\circ$ ) with the CdS compensator, no sample in the beam, and measure maximum and minimum intensities defined as  $I_{\text{max}}^1$  and  $I_{\text{min}}^1$  as shown in Fig. 3(b) from the chart recorder output. Now we can write

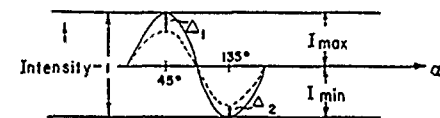
$$\cos\delta_c = 1 - (\Delta_1^c + \Delta_2^c), \quad (16)$$

when from Fig. 3(b) we find

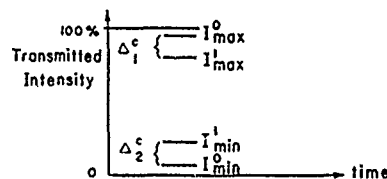
$$\Delta_1^c = \frac{I_{\text{max}}^0 - I_{\text{max}}^1}{I_{\text{max}}^0 - I_{\text{min}}^0}, \quad \Delta_2^c = \frac{I_{\text{min}}^0 - I_{\text{min}}^1}{I_{\text{max}}^0 - I_{\text{min}}^0}. \quad (17)$$

Inserting Eq. (17) into Eq. (16) and simplifying, one gets

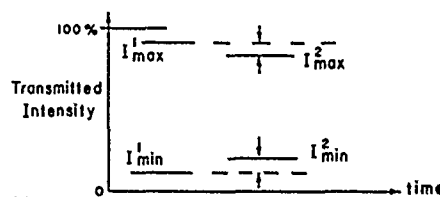
$$\cos\delta_c = \frac{I_{\text{max}}^1 - I_{\text{min}}^1}{I_{\text{max}}^0 - I_{\text{min}}^0}. \quad (18)$$



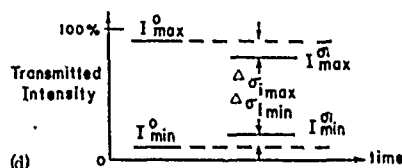
(a)



(b)



(c)



(d)

FIG. 3. (a) Variation of measured intensity with azimuth angle  $\alpha_2$  of the analyzer for a fixed retardance  $\delta$ . (b) Intensity measurements for fixed  $\alpha_1$ ,  $\alpha_2$ , and  $\delta_c$ ; no sample in beam. (c) Intensity measurements with added retardance and sample in beam. (d) Intensity measurements with compensator and stressed sample in beam.

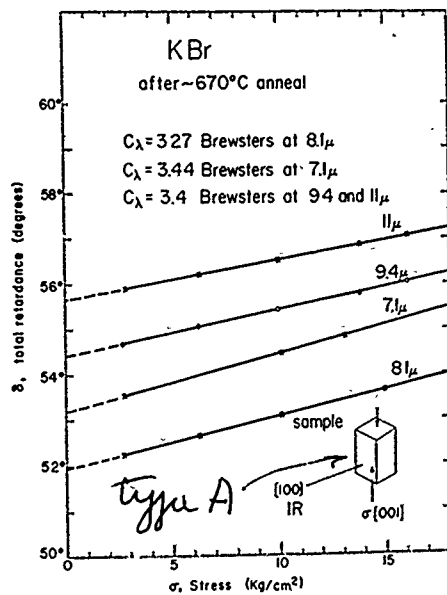


FIG. 4. Relative total retardance vs stress for KBr at wavelengths shown.

In this third step we set  $\alpha_2 = 90^\circ$  for the analyzer and now the intensity will be  $I = \frac{1}{2}(I_{\max}^1 + I_{\min}^1)$ . The sample is inserted in the beam and the intensity reading (on the recorder) is brought electronically back ( $\approx 3\%$ ) to the point for intensity  $I$ . By setting  $\alpha_2 = 45^\circ$  and  $135^\circ$ , respectively, we obtain the intensities  $I_{\max}^2$  ( $\alpha_2 = 45^\circ$ ) and  $I_{\min}^2$  ( $\alpha_2 = 135^\circ$ ) these typical results are as shown schematically in Fig. 3(c). Following the same procedure by which we obtained Eq. (18) we can now write

$$\cos(\delta_c + \delta_r) = \frac{I_{\max}^2 - I_{\min}^2}{I_{\max}^0 - I_{\min}^0} \quad (19)$$

The retardance in Eq. (19) includes that due to the compensator,  $\delta_c$ , which is known, plus  $\delta_r$ , the unknown retardance due to residual stress in the sample. In the fourth and final step the electronic amplifier gain is expanded to a sufficient value to enable us to obtain  $I_{\max}^2$  ( $\alpha_2 = 45^\circ$ ), or  $I_{\min}^2$  ( $\alpha_2 = 135^\circ$ ). Then successively higher stresses are applied to the sample,  $\sigma_1, \sigma_2, \sigma_3, \dots$ , all of which are within the linear stress-strain range for the material, and we obtain the corresponding intensities  $I_{\max}^2, I_{\min}^2, I_{\max}^2, \dots$  etc., which lead to an expression for the retardance angle in the same way Eq. (19) was derived:

$$\cos(\delta_r) = \frac{I_{\max}^2 - I_{\min}^2}{I_{\max}^0 - I_{\min}^0} \quad (20)$$

These typical results are shown schematically in Fig. 3(d). We usually find  $\Delta\sigma_{I_{\max}^2} \approx \frac{3}{2} \Delta\sigma_{I_{\min}^2}$  and measurements are made with  $\sigma_1 < \sigma_2 < \sigma_3 \dots < \sigma_{\max}$ ,  $\sigma_{\max} < \sigma$ , the elastic limit. The retardance angle  $\delta$  and stress optic coefficient  $C_\lambda$  are defined as  $\delta = [(n_1 - n_2)/\lambda] \alpha \times 360^\circ$  and  $C_\lambda = (n_1 - n_2)/\sigma$ , respectively,  $n_1$  and  $n_2$  are the ordinary and extraordinary indices of refraction. Therefore, under our experimental conditions we can write the

retardance angle  $\delta$  in terms of stress  $\sigma$  and sample dimension  $a$  [see Fig. 1(a)] as follows:

$$\lambda\delta/360 = C_\lambda \sigma a, \quad (21)$$

$$\delta = (360aC_\lambda/\lambda)$$

and from the slope of a  $\delta$  versus  $\sigma$  plot  $C_\lambda$  is obtained.

The importance of having optimum signal to noise comes from the fact that the measured values of  $\Delta\sigma_i$  [Fig. 3(d)] are very small for the alkali halides (signal  $\sim 100$ – $300$  nV or  $\approx 0.2\%$  of full scale).

#### IV. RESULTS AND DISCUSSIONS

##### A. Alkali halides

In Fig. 4 we present results on the behavior of retardance  $\delta$ , as a function of stress  $\sigma$  for KBr at various wavelengths from  $8.1$  to  $11 \mu\text{m}$ . The sample shown in Fig. 4 was annealed to  $\approx 680^\circ\text{C}$  for several hours then slow cooled to room temperature. The cool-down time was about 10 h. This heat treatment was found to reduce the retardance due to residual stress  $\approx 2$ – $3^\circ$ , and did not cause any discoloration of the sample. A slight yellow color was observed on one sample given similar heat treatment. The slopes of the lines in Fig. 4 which are the stress optic coefficient  $C_\lambda$  [for our case  $C_\lambda = \frac{1}{2}n_0^3(q_{11} - q_{12})$ ] all yield the constant values  $+3.3 \pm 0.1$  Brewster.

Our stress optic results for KCl in the  $4.6$ – $11 \mu\text{m}$  wavelength range are shown in Fig. 5. This sample was also heat treated to  $\approx 680^\circ\text{C}$  similar to the KBr sample of Fig. 4. The measurements for both KBr and KCl were made with light incident in the  $[100]$  direction and sample stressed in the  $[010]$  direction which results in a  $C_\lambda$  as given above.

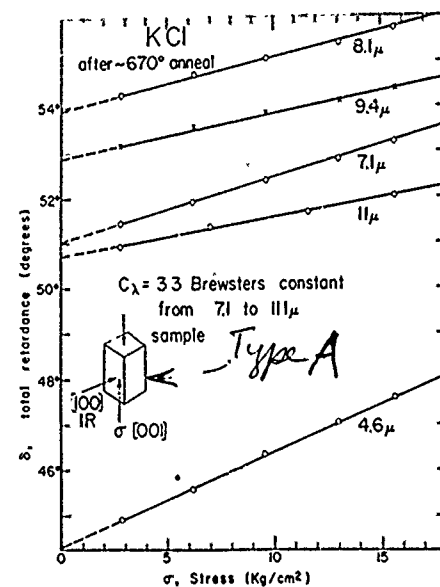


FIG. 5. Relative total retardance vs stress for KCl at wavelengths shown.

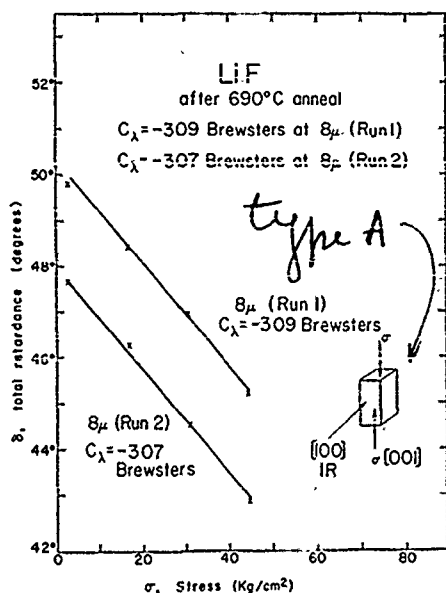


FIG. 6. Relative total retardance vs stress for LiF at  $8 \mu\text{m}$ .

From the KCl results of Fig. 5 we obtain a slope which yields a  $C_\lambda$  of  $+3.3 \pm 0.1$  Brewsters. By making repeated measurements and checking our results with at least two different samples we estimate our maximum error to be  $\pm 10\%$ . The value of  $C_\lambda$  we obtain for KCl is within experimental error of the value  $\pm 3.00$  Brewsters reported by Wilkening *et al.*<sup>20</sup> at  $0.6328 \mu\text{m}$ . Our value is about 16% higher than the measurement of Bhagavantam and Murty<sup>21</sup> at  $\approx 0.63 \mu\text{m}$  who reported  $C_\lambda = +2.75$  Brewsters.

We also include results on a LiF crystal whose stress birefringence was measured at  $8 \mu\text{m}$  and is shown in Fig. 6. Two runs were made at  $8 \mu\text{m}$  on two consecutive days from which the values obtained were  $-3.07$  and  $-3.09$  Brewsters, respectively. The value reported by Wilkening *et al.*<sup>20</sup> at  $0.6328 \mu\text{m}$  was  $-2.88$  Brewsters and represents a difference of about 30% in the two measurements which is outside the experimental error. The results indicate that LiF has a more pronounced wavelength dependence in the  $0.6$ – $8$ - $\mu\text{m}$  region than either KCl or KBr. The latter two alkali halides appear to exhibit little or no dependence of  $C_\lambda$  on the wavelength in the range  $0.6$ – $11 \mu\text{m}$ . As we compare the  $C_\lambda$  results for KCl, KBr, and LiF (see Figs. 4–6) we see that the slope of the  $\delta$  versus- $\sigma$  plot is negative for the LiF material which gives a negative value of stress optic coefficient.

The points at  $\sigma = 16 \text{ kg/cm}^2$  in the  $\delta$ -versus- $\sigma$  plot for the KBr and KCl (Figs. 4 and 5) fall on a straight line which indicates that we are still within the elastic limit. The retardance angle  $\delta$  ranges from  $2.5^\circ$  to  $1.5^\circ$  for  $4.6$  to  $11 \mu\text{m}$ , respectively at  $\sigma = 16 \text{ kg/cm}^2$ . It is therefore almost impossible to measure without adding the CdS compensator in front of the sample. It is clear from the results shown in Figs. 4 and 5 that the retardance  $\delta$  decreases as we increase the wavelength from  $4.6$  to  $11 \mu\text{m}$ . Therefore, we must conclude that the stress

optic coefficients for the alkali halide crystals exhibit very little or no dependence on the wavelength in the range from  $0.6$  to  $11 \mu\text{m}$ . The difference in values between  $0.633 \mu\text{m}$  and the infrared region could be attributed to the experimental errors due to two measurements.

## B. Polycrystalline ZnS

The stress birefringence of several specimens of polycrystalline ZnSe grown by chemical vapor deposition (CVD) was studied in the  $9.4$ – $11$ - $\mu\text{m}$  wavelength range. The samples were not given any heat treatment prior to measurement of  $C_\lambda$ . Since the material is grown slowly by CVD we expect relatively low residual strain in the material. In hot-pressed ZnSe material we determined from strain patterns by the crossed-polarizer method that the approximate upper limit of the yield stress was  $\sim 50 \text{ kg/cm}^2$ . Therefore in our measurements we kept the stress on the sample during measurement below  $18 \text{ kg/cm}^2$  to ensure that we were stressing within the elastic limit. Retardance-versus-stress results for ZnSe sample No. 2A are given at  $9.4$  and  $11 \mu\text{m}$  in Fig. 7. In similar results for another sample of ZnSe cut from a different portion of the ingot we obtain  $C_\lambda$  values which are 15–30% lower. These differences lie outside the maximum experimental error and probably are due to inhomogeneities in different parts of the ZnSe ingot grown by chemical vapor deposition.

From Fig. 7 we can see that polycrystalline ZnSe shows a negative sign for the stress optic coefficient and is constant in the  $9$ – $11$ - $\mu\text{m}$  wavelength region.

## ACKNOWLEDGMENTS

The initial impetus to perform the research reported in this paper was provided by Dr. Carl Pitha and Dr.

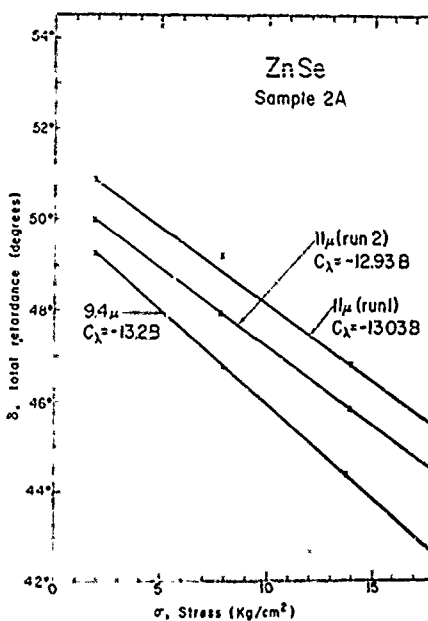


FIG. 7. Relative total retardance vs stress for ZnSe sample No. 2A at wavelengths shown.

Lyn Skolnik of the U. S. Air Force Cambridge Research Laboratories, Bedford, Massachusetts. They also provided the authors with all sample specimens used in this study and informed them of the method of measuring the stress optic coefficient. The authors have also benefited greatly from discussions with Welden Wilkening in the early stages of the work, and Jerry Friedman at the completion of the experiments. They also thank Charles Clahasey for help in sample preparation and for making some of the first measurements. Thanks are due to Dr. E. D. Palik of the U. S. Naval Research Laboratories for the loan of his CdS Soleil compensator.

<sup>†</sup>Research supported by the U. S. Air Force Cambridge Research Laboratories, Bedford, Mass.

\*Present address: Birroughs Cor., 16701 West Bernardo Drive, San Diego, Calif. 92127.

<sup>†</sup>To whom reprint requests should be made.

<sup>1</sup>K. G. Bansigir and K. S. Iyengar, Proc. Phys. Soc. Lond. 71, 225 (1958).

<sup>2</sup>R. Srinivasan, Z. Phys. 155, 281 (1959).

<sup>3</sup>K. Veerabhadra Rao and T. S. Narasimhamurty, Appl. Opt. 9, 155 (1970).

<sup>4</sup>A. H. Rahman and K. S. Iyengar, Acta Crystallogr. 20, 144 (1966).

<sup>5</sup>A. Rahman and K. S. Iyengar, Phys. Lett. A 25, 478 (1967).

<sup>6</sup>A. H. Rohman and K. S. Iyengar, Acta Crystallogr. A 26, 128 (1970).

<sup>7</sup>A. Feldman, Phys. Rev. 150, 748 (1966).

<sup>8</sup>A. Feldman and D. Horowitz, Solid State Commun. 6, 607 (1968).

<sup>9</sup>A. Feldman and D. Horowitz, J. Appl. Phys. 39, 5597 (1968).

<sup>10</sup>R. M. Waxler and E. N. Farabaugh, J. Res. Natl. Bur. Stand. A. 74, 215 (1970).

<sup>11</sup>A. A. Giardini and E. Poindexter, J. Opt. Soc. Am. 48, 556 (1958).

<sup>12</sup>R. M. Waxler, G. W. Cleek, I. H. Malitson, M. J. Dodge, and T. A. Hahn, J. Res. Natl. Bur. Stand. A 75, 163 (1971).

<sup>13</sup>A. J. Michael, J. Opt. Soc. Am. 58, 889 (1968).

<sup>14</sup>H. Mueller, J. Opt. Soc. Am. 38, 661 (1948).

<sup>15</sup>R. Soleillet, Ann. Phys. (Paris) 12, 23 (1929).

<sup>16</sup>E. D. Palik and B. W. Henvis, Appl. Opt. 6, 2198 (1967).

<sup>17</sup>B. H. Billings and E. H. Land, J. Opt. Soc. Am. 38, 819 (1948).

<sup>18</sup>M. J. Walker, Am. J. Phys. 22, 170 (1954).

<sup>19</sup>The KBr, CKI, and LiF samples were grown by personnel of the Solid State Sciences Laboratory, U. S. Air Force Cambridge Research Laboratories, Bedford, Mass.

<sup>20</sup>W. W. Wilkening, J. Friedman, and C. A. Pitha (private communication).

<sup>21</sup>S. Bhagavantam and Y. K. Murty, Proc. Ind. Acad. Sci. A 46, 339 (1957).